

## Electrochemical Sensors based on Fe@Fe<sub>2</sub>O<sub>3</sub> nanowires, N-Doped ZnO and Au nanoparticles for quercetin determination

Danping Xie, Xiaoli Guo, pengna Li, Wenxin Zhang, Yanyan Shao, yingjuan Qu, yunhui Zhai

College of Chemical Engineering, Xi'an University, Xi'an, Shaanxi 710065, China

\*E-mail: [xdp819@163.com](mailto:xdp819@163.com)

Received: 7 June 2022 / Accepted: 16 September 2022 / Published: 10 October 2022

In this study, we developed an electrochemical sensor for the determination of quercetin (QR) based on nitrogen-doped zinc oxide (N-ZnO) and iron/iron(III) oxide(Fe@Fe<sub>2</sub>O<sub>3</sub>) nanowires and gold nanoparticles (AuNPs). N-ZnO nanomaterial was decorated onto the indium tin oxide (ITO) surface by high-temperature catalytic oxidation while AuNPs and Fe@Fe<sub>2</sub>O<sub>3</sub> were prepared using the hydrothermal method and were then coated on N-ZnO/ITO electrode by drop-casting method to form Fe@Fe<sub>2</sub>O<sub>3</sub>/AuNPs/N-ZnO/ITO electrode. The electrochemical oxidation of QR at the Fe@Fe<sub>2</sub>O<sub>3</sub>/AuNPs/N-ZnO/ITO electrode was studied by cyclic voltammetry. It was found that the oxidation current of QR was significantly enhanced at the Fe@Fe<sub>2</sub>O<sub>3</sub>/AuNPs/N-ZnO/ITO electrode. By taking advantage of high surface area and good electron transfer of the nanomaterials, as well as the electrochemical oxidation reaction of QR, an electrochemical method was developed for the detection of QR with a linear range from 10 to 1000 μM (R<sup>2</sup>=0.961) and the limit of detection of 0.059 mM. This work provides a new electrochemical method for the detection of QR with improved performance by constructing an advanced electrochemical sensing platform.

**Keywords:** Fe@Fe<sub>2</sub>O<sub>3</sub>, N-ZnO, quercetin, electrochemical method

### 1. INTRODUCTION

Zinc oxide (ZnO) is a typical broad-band (3.37 eV) semiconductor material with many excellent properties[1], such as good electron mobility, high surface area, high stability, and adequate biocompatibility[2-3]. For these advantages, ZnO has been applied to water splitting[4-6], sensors[7-8], lithium-ion batteries, fuel cells, and supercapacitors. However, it is noted that the application of ZnO was restricted by the low conductivity and limited charge communication [9]. In order to improve electrocatalytic capacity and accelerate the direct electron transfer, chemical doping may be used. Nitrogen is one of the most widely used dopant and has been studied to modify the magnetic and electronic properties of ZnO[10-11]. In addition, Fe<sub>2</sub>O<sub>3</sub> is another potential material with a narrow gap

of 2.21 eV[12]. Fe<sub>2</sub>O<sub>3</sub> has the advantages of high stability under alkaline conditions, low cost, easy availability, and environmentally friendly[13-16].

Quercetin (QR) is one of the representative substances of polyphenolic compounds, which has chemopreventive and therapeutic effects on various diseases. Quercetin has bioactive qualities, including anti-cancer, anti-virus, and antioxidant properties[17]. QR can also protect human colon cells from in vitro oxidation and can act as a substance that blocks oxidative damage to DNA to prevent mutations in the organism[18]. Therefore, the detection of QR is of great significance to human health. Generally, QR has been detected using spectrophotometry[19], fluorescence[20], high-performance liquid chromatography, capillary electrophoresis[21], and electrochemical methods[22]. Among these techniques, Electrochemical method is widely used in the analysis and detection of QR due to their simplicity and high sensitivity.

In this work, a new electrochemical sensor for the determination of QR based on nitrogen-doped zinc oxide (N-ZnO) and iron/iron(III) oxide(Fe@Fe<sub>2</sub>O<sub>3</sub>) nanowires and gold nanoparticles (AuNPs) was developed. N-ZnO nanomaterial was decorated onto the indium tin oxide (ITO) surface by high-temperature catalytic oxidation method. AuNPs and Fe@Fe<sub>2</sub>O<sub>3</sub> were prepared using the hydrothermal method and were then coated on N-ZnO/ITO electrode by drop-casting method. Compared with the electrochemical method based on ZnO and Fe<sub>3</sub>O<sub>4</sub> nanoparticles, the electrochemical method based on Fe@Fe<sub>2</sub>O<sub>3</sub> nanowires, N-ZnO, and AuNPs modified ITO shows a wider linear range and higher sensitivity for the detection of quercetin.

## 2. EXPERIMENTAL

### 2.1 Material and Methods

Cycle voltammetry (CV) measurements were performed at a LK2005A electrochemical workstation (Tianjin Lanlike Instrument, China). Other instruments used include a DHG-9053A Series Heating and Drying Oven (Qixin Scientific Instrument, Shanghai, China), KSL-1200X-J Muffle furnace (Kejing Technology Material, Hefei, China), GL124-1SCN analytical balance (Sartorius, Sartorius Group, Beijing, China), and LP-500 photocatalytic apparatus (Lanmiao, Shanghai, China).

A conventional three-electrode system was conducted with a platinum wire as auxiliary electrode, a saturated Ag/AgCl as reference electrode and the modified ITO electrode (75×15 mm) as the working electrode. All reagents were analytically pure. The 0.1 M phosphate buffer solution (pH 7.4) was prepared from disodium phosphate (Na<sub>2</sub>HPO<sub>4</sub>) and monosodium phosphate (NaH<sub>2</sub>PO<sub>4</sub>) (Sigma-Aldrich), which was adjusted to 7.0 by phosphoric acid (H<sub>3</sub>PO<sub>4</sub>) and sodium hydroxide (NaOH). Ultrapure water, which was produced by the Millipore system, was used for all experiments. Zinc acetate (Zn(Ac)<sub>2</sub>, ω% ≥ 99.0) and ammonium nitrate (NH<sub>4</sub>NO<sub>3</sub>) were purchased from Sinopharm Chemical Reagent Co., Ltd. The QR was obtained from Shengong Biological Engineering, Shanghai, China.

Reagent	Manufacturer
ethanol, acetone, (3-Aminopropyl)triethoxysilane(APTES), glutaraldehyde, NaOH, H <sub>3</sub> PO <sub>4</sub> , iron(III) triperchlorate (Fe(ClO <sub>4</sub> ) <sub>3</sub> ), sodium borohydride (NaBH <sub>4</sub> ), chloroauric acid (HAuCl <sub>4</sub> ), trisodium citrate (C <sub>6</sub> H <sub>5</sub> Na <sub>3</sub> O <sub>7</sub> ), ammonium nitrate (NH <sub>4</sub> NO <sub>3</sub> )	Sinopharm Chemical Reagent Co., Ltd.
indium tin oxide (ITO)	South China Xiangcheng Technology Co., Ltd.

### 2.2 Preparation of the Fe@Fe<sub>2</sub>O<sub>3</sub>/AuNPs/N-ZnO/ITO electrode

The Fe@Fe<sub>2</sub>O<sub>3</sub>/AuNPs/N-ZnO/ITO electrode was prepared as following. It was reported that doping of ZnO nanoparticles can be achieved by loading with noble metal nanoparticles (e.g. Pd, Pt, Au) to improve active site immobilization [23-25]. First, an ITO surface (75×15×1.1 cm, 15 Ω) was used as base electrode and was cleaned by sonication in acetone, isopropanol, and absolute ethanol for 20 minutes and was dried in a vacuum oven before use. N-ZnO nanomaterial was decorated onto the indium tin oxide (ITO) surface by high-temperature catalytic oxidation method. The mixed solution of Zn(Ac)<sub>2</sub> and NH<sub>4</sub>NO<sub>3</sub> was prepared at equal molar concentrations (0.5 mM) of 50 μL. Then, 10 μL Zn(Ac)<sub>2</sub>-NH<sub>4</sub>NO<sub>3</sub> suspension was drop-coated on the ITO surface. It was calcined at 450°C for 2 h to form N-ZnO/ITO.

Fe@Fe<sub>2</sub>O<sub>3</sub> core-shell nanowires were prepared [26]. 0.012 M Fe(ClO<sub>4</sub>)<sub>3</sub> was added into a 0.4 M NaBH<sub>4</sub> solution dropwise while stirring at 0.5 mL/s, until the mixture turned into a black flocculent precipitate and produced a lot of bubbles. The resulting solution stood for 2–3 h. The above products were washed several times with water and ethanol. The products were then dried using infrared light in a vacuum-drying oven to get Fe@Fe<sub>2</sub>O<sub>3</sub> core-shell nanowires. The Fe@Fe<sub>2</sub>O<sub>3</sub> (15 mg) was dispersed in 5 mL of ethanol and stirred for 5 minutes. AuNPs were prepared by stirring 0.25 mM HAuCl<sub>4</sub> and 20 mg/mL trisodium citrate solution for 30 minutes while being heated. The AuNPs size was 20 nm. Then, 100 μL of AuNPs and Fe@Fe<sub>2</sub>O<sub>3</sub> suspension was drop-casted on the N-ZnO/ITO electrode and then dried in the oven to get Fe@Fe<sub>2</sub>O<sub>3</sub>/AuNPs/N-ZnO/ITO electrode.

### 2.3 Electrochemical detection

10 μL 10% APTES solution was added into Fe@Fe<sub>2</sub>O<sub>3</sub>/AuNPs/N-ZnO/ITO electrode at room temperature for 1 h and rinsed with ethanol. Afterwards, 50 μL glutaraldehyde solution (2.5%) was dropped onto the modified electrode for 2 h at room temperature and washed with water. The modified electrodes were incubated with 10 mM QR in 0.1 M PBS (pH 7.0) overnight at 4°C. Electrochemical detection was performed using CV technique.

### 3. RESULTS AND DISCUSSION

#### 3.1 Electrochemical behavior of quercetin at modified electrode

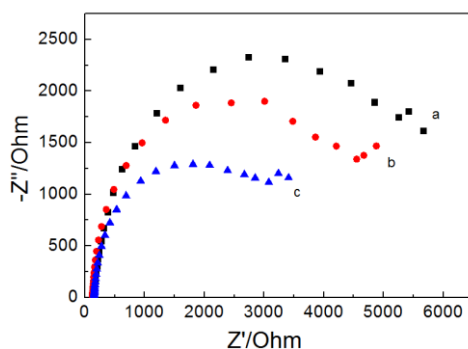


**Figure 1.** Nyquist plots from the electrochemical impedance measurements of different modified electrode. (a) N-ZnO/ITO, (b) AuNPs/N-ZnO/ITO, (c) Fe@Fe<sub>2</sub>O<sub>3</sub>/AuNPs/N-ZnO/ITO.

The assembly process of the electrochemical sensor was confirmed with electrochemical impedance spectroscopy (EIS) by investigating in 0.1 M potassium chloride containing 5 mM ferricyanide Fe(CN)<sub>6</sub><sup>3-/4-</sup> (Fig. 1). Compared with the N-ZnO/ITO electrode (curve a), the radius of AuNPs/N-ZnO/ITO (curve b) decreased, indicating faster electron transfer. This can be ascribed to the impact of the AuNPs immobilization on the electrode surface. Then, the  $R_{et}$  value further decreased when Fe@Fe<sub>2</sub>O<sub>3</sub> was added on the AuNPs/N-ZnO/ITO electrode (curve c) due to the nanoscale zerovalent iron (nZVI) of Fe@Fe<sub>2</sub>O<sub>3</sub> and its reduction properties [27].

The electrochemical responses of the QR at Fe@Fe<sub>2</sub>O<sub>3</sub>/AuNPs/N-ZnO/ITO electrode was investigated by cyclic voltammetry between -0.3 to 0.8 V in 0.1 M PBS (pH 7.0) at a scan rate of 100 mV/s. Fig. 2 shows that the currents gradually increase as the electrode material layer increases. This phenomenon may be caused by the N-ZnO mesoporous construction, which assembled more nanomaterials on the electrode surface. The core-shell structure of Fe@Fe<sub>2</sub>O<sub>3</sub>, which is nZVI, possesses the characteristics of reducibility and large specific surface area, which can accelerate charge transfer [28]. There are three possible reasons for the current rapidly increasing on the electrode. One possibility is that, under electrochemical conditions, the zero-valent iron in the core-shell Fe@Fe<sub>2</sub>O<sub>3</sub> may oxidize the hydroxyl groups at the 3' and 4' positions (Fig. 3) of QR [29], which promotes the transfer of electrons on the electrode. Another possibility is that the unencapsulated zero-valent iron in Fe@Fe<sub>2</sub>O<sub>3</sub> can form a metal chelate with QR, which increases the amount of QR on the electrode surface [30]. In general, the enhanced effect of Fe@Fe<sub>2</sub>O<sub>3</sub>/Au/N-ZnO/ITO on QR oxidation may be related to the composite superposition and structure.

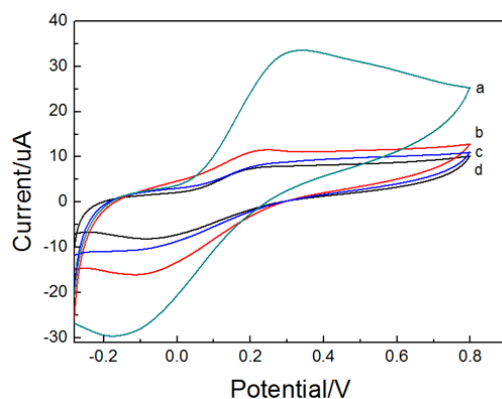


**Figure 2.** Cyclic voltammograms of QR at different electrodes in 0.1 M PBS (pH 7.0) containing 1mM QR. (a) Fe@Fe<sub>2</sub>O<sub>3</sub>/AuNPs/N-ZnO/ITO, (b) AuNPs/N-ZnO/ITO, (c) N-ZnO/ITO, (d) ZnO/ITO.

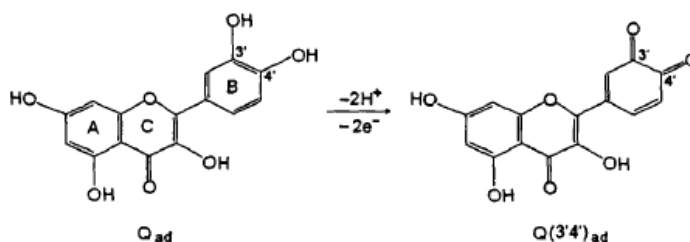


**Figure 3.** Schematic mechanism of electrochemical oxidation of QR

### 3.2 Factors affecting electrochemical behavior of quercetin at modified electrode

The pH of the buffer solution has an important effect on the electrochemical response of QR on the Fe@Fe<sub>2</sub>O<sub>3</sub>/AuNPs/N-ZnO/ITO electrode. The N-ZnO is an amphoteric compound that is unstable in strong acid and base solutions. Therefore, we adopted the pH value range from 3 to 8 to study the effect of pH on the oxidation current of QR. Fig. 4 (A) shows the relationship between the current and pH. The current gradually increased between pH 3 to 7; however, when it exceeded 7, the current decreased. The pH of buffer solution was optimized to 7.0 in the following experiment.

The effect scan rate on the oxidation current of QR was examined between 40 to 100 mV/s using CV as shown in Fig. 4(b). It can be seen that the oxidation peak currents gradually increased with the scan rate increased between 40 and 100 mV/s (Fig. 4(b)). It is noted clearly that the peak current was linearly related to the scan rate. The electrochemical reaction of QR at Fe@Fe<sub>2</sub>O<sub>3</sub>/AuNPs/N-ZnO/ITO electrode is an absorption controlled process [31].

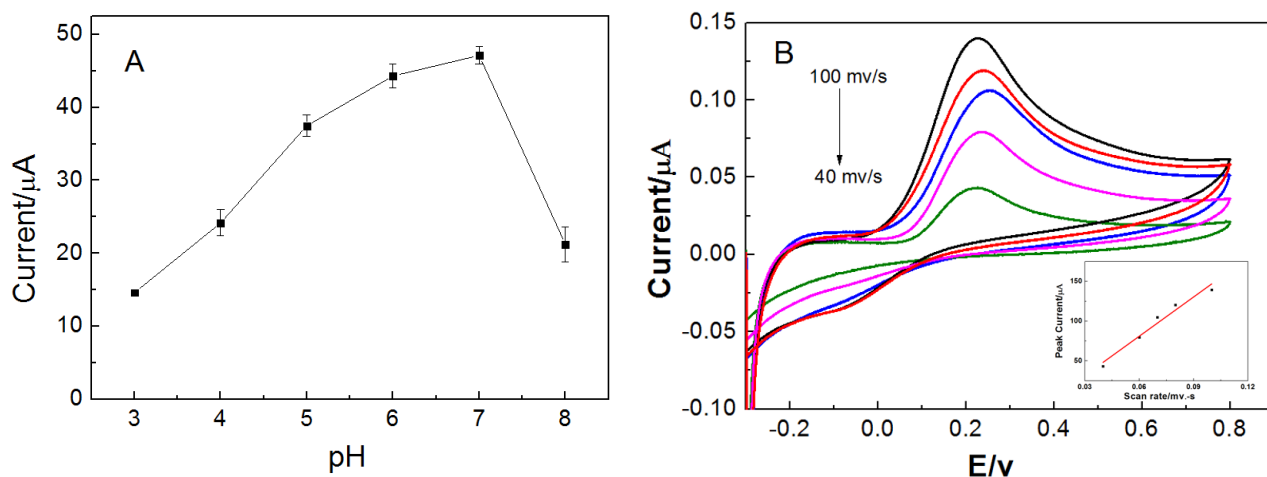


**Figure 4.** The effect of pH (A) and scan rate (B) on the oxidation current of QR at Fe@Fe<sub>2</sub>O<sub>3</sub>/AuNPs/N-ZnO/ITO.

The sensor performance of QR at the prepared Fe@Fe<sub>2</sub>O<sub>3</sub>/AuNPs/N-ZnO/ITO electrode was investigated. CVs were recorded at the Fe@Fe<sub>2</sub>O<sub>3</sub>/AuNPs/N-ZnO/ITO electrode with the different concentrations of QR. The concentration of QR increased from 10 μM to 4000 μM.

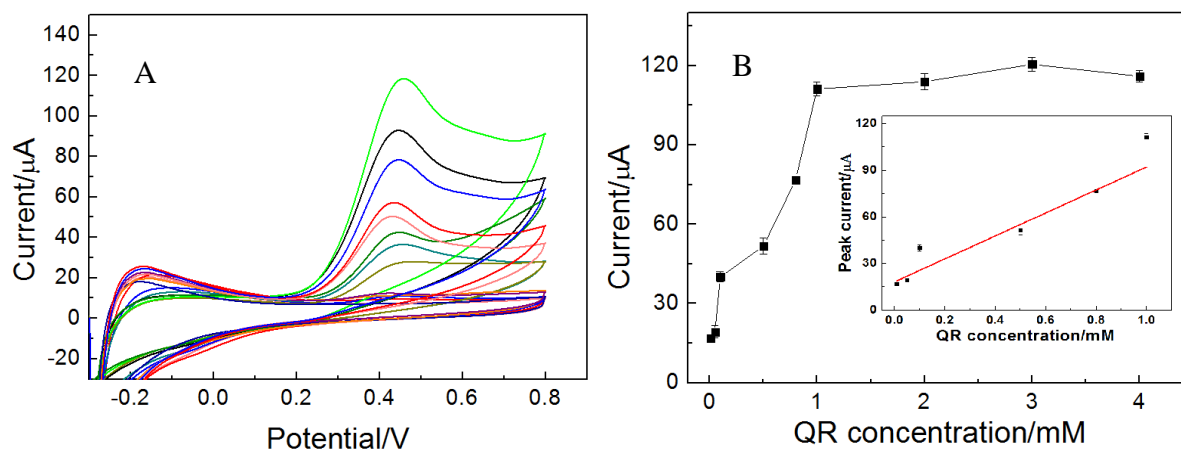


**Figure 5.** Cyclic voltammograms of QR at different concentrations at Fe@Fe<sub>2</sub>O<sub>3</sub>/AuNPs/N-ZnO/ITO in PBS at a scan rate of 0.1 V/s ( $C_{QR}$ : 10~4000 μM). (B) The relationship between the oxidation current and QR concentration. Insert, Calibration curve of QR.

The obtained CVs at the Fe@Fe<sub>2</sub>O<sub>3</sub>/AuNPs/N-ZnO/ITO electrode is shown in Fig. 5(A). The current increased as the QR concentration increased from 10 μM to 4000 μM, then saturated. Fig. 5(b) shows the relationship between the QR concentrations and oxidation current. As can be seen from Fig. 5(b) inset, the calibration curve of QR concentration was observed in the range from 10 to 1000 μM ( $R^2=0.961$ ). The linear equation was  $I=73.933c+18.250$ , and the limit of detection was 0.059 mM. The oxidation current at low concentration exhibits much larger fluctuation as compared to at higher

concentrations. The analytical performance of this method is compared with some previously reported studies, and the comparison results are summarized in Table 1. By comparison, the Fe@Fe<sub>2</sub>O<sub>3</sub>/AuNPs/N-ZnO/ITO-modified electrode has outstanding performance in QR detection. This result indicates that the Fe@Fe<sub>2</sub>O<sub>3</sub>/AuNPs/N-ZnO/ITO electrode for QR exhibited good sensitivity and therefore provides a potential sensor platform.

**Table 1.** Comparison of analytical method of Fe@Fe<sub>2</sub>O<sub>3</sub>/AuNPs/N-ZnO/ITO with previous studies for the QR determination.

Modified electrode	LOD/mM	Linear range/ $\mu$ M	Reference
Poly-AMT/PGE	2.2	0.33–19.83	29
FCo-NP/GCE	0.1	0.5–330	30
PVP/CPE	0.17	0.5–5.5	31
Fe <sub>3</sub> O <sub>4</sub> @ZnO/CP/GCE	0.159	0.79–61.01	32
Fe <sub>3</sub> O <sub>4</sub> @ $\beta$ -CD-WMCNTs/SPE	0.084	0.95–100	33
Fe@Fe <sub>2</sub> O <sub>3</sub> /AuNPs/N-ZnO/ITO	0.059	10–1000	This work

### 3.3 Stability and repeatability of the electrochemical sensor

The repeatability of the modified electrode was investigated by CV. In our experiment, six working electrodes were fabricated under the same conditions for the detection of 1 mM QR in PBS. The electrochemical experiment demonstrated parallel responses with relative standard deviation (RSD) of 2.17%. The modified electrode preserved 93.1% of its activity current response after five weeks when kept at 4°C. The results indicated that this electrochemical method could be used for QR detection with good stability.

### 3.4 Detection results of QR samples

The reliability analysis of this electrochemical sensor was evaluated by recovery experiments. The QR detection data of Jiangzhining particles shows in Table 2. With absolute ethanol as the extractant, the volume ratio of Jiangzhining particles and the extract solution was 1:40. After sonicating for 25 min, the mix solution was stand and took the supernatant. The liquid supernatant was filtered with 0.22  $\mu$ m membrane. The CV responses of Jiangzhining particles shows the recovery in the range of 90.0% and 104% with RSDs of 3.2% to 4.9%, respectively. Our data results indicated the method was suitable for QR determination in medicine.

**Table 2.** QR detection results of Jiangzhining particles (n=3)

Sample number	Added( $\mu\text{M}$ )	Found ( $\mu\text{M}$ )	Recovery(%)	RSD(%)
1	10	9.0	90	4.8
2	50	48.0	96	4.9
3	100	104	104	3.2
4	500	508	101	4.6
5	800	803	100	3.5

#### 4. CONCLUSIONS

In summary, a sensitive electrochemical sensor for the detection of QR was developed based on N-ZnO nanoparticles and Fe@Fe<sub>2</sub>O<sub>3</sub> nanowires and AuNPs. Mesoporous structure of N-ZnO has higher specific surface area on electrode, the electrical conductivity of N-ZnO and AuNPs can increase the electron transfer of QR. With our design, the developed sensor displayed high sensitivity good linear range and good stability for QR detection. This strategy provides a promising electrochemical method for QR detection with high sensitivity and good stability.

#### ACKNOWLEDGEMENTS

The author thanks Prof. PengNa Li, Xi'an University, for providing Fe@Fe<sub>2</sub>O<sub>3</sub> synthesis in this work. This study was financially supported by the Scientific Research Project Foundation of Xi'an University [No. 2020KJWL25] and Xi'an Key Laboratory of Food Safety Testing and Risk Assessment.

#### References

1. S. Cho, J.W. Jang, J.S.Lee, *Nanoscale*, 4 (2012) 2066.
2. Y.F. Wei, L. Ke, E.S. P. Leong, H.Liu, L.L.Liew, J.H.Teng, H.j. Du and X. W.Sun, *Nanotechnology*, 23 (2012) 365704.
3. K.S. Ahn, S. Shet, T. Deutsch, Ch.Sh. Jiang, Y.F.Yan, M.A.Jassim and J.Turner, *J. Power Sources*, 176(2008) 387.
4. W.J. Jian, X.L. Cheng, Y.Y.Huang and Y.You, *Chem. Eng. J*, 328 (2017) 474.
5. W.W. Zhang, W.Zh.Wang H.L.Shi, Y.J. Liang,J.L.Fu and M.Zhu, *Sol. Energy Mater. Sol. Cells*, 180 (2018) 25.
6. G.M. Wang, Y. Ch. Li and Yat Li, *Nanoscale*, 4 (2012) 6682.
7. W. Raza and K.Ahmad, *Mater. Lett.*, 212 (2018) 231.
8. W. Liu, W.T. Zhan, X.Y. Jia, Q. Liu, R. Sh.Chen, D. Li, Y. Huang, G.Y. Zhang and H.W. Ni, *Appl Surf. Sci*, 480 (2019) 341.
9. K. Arora, M. Tomar and V.Gupta, *Biosens. Bioelectron.*, 30 (2011) 333.
10. K. Jindal, M. Tomar, R.S. Katiyar and V. Gupta, *J. Appl. Phys.*, 111 (2012) 102805.
11. L. Liu, J.L. Xu, D.D. Wang, M.M. Jiang, Sh.P. Wang, B.H. Li, Z.Z. Zhang, D. X. Zhao, C.X. Shan, B. Yao and D. Z. Shen, *Phys. Rev. Lett*, 108 (2012) 215501.
12. D. Barreca, G. Carraro, A. Gasparotto, Ch. Maccato, M.E.A. Warwick, K. Kaunisto, C. Sada, S. Turner, Y. Gönüllü, T. Ruoko, L. Borgese, E. Bontempi, G.V. Tendeloo, H. Lemmetyinen and S.



- Mathur, *Adv. Mater. Interfaces*, 2 (2015) 1500313.
13. P. S. Bassi, X.L. Li, Y.N. Fang, J.S. Ch. Loo, J. Barber and L.H. Wong, *Phys. Chem. Chem. Phys.*, 16 (2014) 11834.
  14. D. A. Wheeler, G. M. Wang, Y. Ch. Ling, Yat Li and J. Z. Zhang, *Energy Environ. Sci.*, 5 (2012) 6682.
  15. B. Iandolo, B. Wickman, I. Zorić and A. Hellman, *J. Mater. Chem. A*, 3 (2015) 16896.
  16. M. Li, J. J. Deng, A. W. Pu, P. P. Zhang, H. Zhang, J. Gao, Y. Y. Hao, J. Zhong and X. H. Sun, *J. Mater. Chem. A*, 2 (2014) 6727.
  17. D. L. Xiao, D. H. Yuan, H. He and M. M. Gao, *J. Lumin.*, 140 (2013) 120.
  18. J. Manokaran, R. Muruganantham, A. Muthukrishnaraj, N. Balasubramanian, *Electrochim. Acta*, 168 (2015) 16.
  19. M. R. Sohrabi and G. Darabi, *Spectrochim. Acta*, Part A, 152 (2016) 443.
  20. T. Asadollahi, Sh. Dadfarnia, A. M. H. Shabani and M. Amirkavei, *J. Food Sci. Technol.*, 52 (2015) 1103.
  21. D. D. Wu and Z. Chen, *J. Biolumin. Chemilumin.*, 29 (2014) 307.
  22. Y. T. Long, Q. L. Hao and X. Chen, *Microchim. Acta*, 181 (2014) 687.
  23. J. Xu, X. Yang, H. K. Wang, X. Chen, Ch. Y. Luan, Z. X. Xu, Zh. Zh. Lu, V. A. L. Roy and Ch. S. Lee, *Nano Lett.*, 11 (2011) 4138.
  24. J. Xu, X. Yang, Q. D. Yang, T. L. Wong, Sh. T. Lee, W. J. Zhang and Ch. S. Lee, *J. Mater. Chem.*, 22 (2012) 13374.
  25. H. Daneshinejad, M. A. Chamjangali, N. Goudarzi and A. Roudbari, *Mater. Sci. Eng., C*, 58 (2016) 532.
  26. P. N. Li, L. Ch. Wang and H. Liu, *Ergonomics J.*, 47 (2018) 1142.
  27. Zh. H. Ai, Zh. T. Gao, L. Zh. Zhang, W. W. He and J. J. Yin, *Environ. Sci. Technol.*, 47 (2013) 5344.
  28. Y. Mu, Zh. H. Ai, L. Zh. Zhang and F. H. Song, *ACS Appl. Mater. Interfaces*, 7 (2015) 1997.
  29. N. Yamashita, H. Tanemura and S. Kawanishi, *Mutat. Res. Fundam. Mol. Mech. Mutagen.*, 425 (1999) 107.
  30. M. Veerapandian, Y. T. Seo, K. Yun and M. H. Lee, *Biosens. Bioelectron.*, 58 (2014) 200.
  31. R. Manjunatha, D. H. Nagaraju, G. S. Suresh, J. S. Melo, S. F. D'Souzac and T. V. Venkateshad, *Electrochim. Acta*, 56 (2011) 6619.

© 2022 The Authors. Published by ESG ([www.electrochemsci.org](http://www.electrochemsci.org)). This article is an open access article distributed under the terms and conditions of the Creative Commons Attribution license (<http://creativecommons.org/licenses/by/4.0/>).